Detection of firearm discharge residue from skin swabs using Trapped Ion Mobility Spectrometry coupled to Mass Spectrometry

Alan McKenzie-Coe,[a] Suzanne Bell,[b] and Francisco Fernandez-Lima[a,c*]

[a]*Department of Chemistry and Biochemistry, Florida International University, Miami, FL 33199, USA. E-mail: fernandf@fiu.edu*

[b] *Professor and Chair, Department of Forensic and Investigative Sciences, West Virginia University, 1600 University Avenue, Oglebay Hall Room 208, Morgantown, WV 26506, USA*

[c]*Biomolecular Science Institute, Florida International University, Miami, FL 33199, USA*

ABSTRACT

In the present work, a novel workflow for the detection of both elemental and organic constituents of the firearm discharge residue from skin swabs was developed using trapped ion mobility spectrometry coupled to mass spectrometry. The small sample size (<10 μL), high specificity and short analysis time (few min) permits the detection of inorganic residues (IGSR; inorganic gunshot residues) and organic residues (OGSR) from one sample and in a single analysis. The analytical method is based on the simultaneous extraction of inorganic and organic species assisted by the formation organometallic complexes (e.g., 15-5 crown ethers for the sequestering of metals and nitrate species), followed by fast, post-ionization, high resolution mobility (R_{IMS} ~150-250) and mass separations (R_{MS} ~ 20-40k) with isotopic pattern recognition. The analytical performance is illustrated as a proof of concept for the case of the simultaneous detection of Ba^{+2}, Pb^{+2}, Cu^{+}, K^{+}, NO_3^{-}, diphenylamine (DPA), ethyl centralite (EC) and 2,4 dinitrotoluene (DNT) in positive and negative nESI-TIMS-MS modes. Candidate structures are proposed and collisional cross sections are reported for all organic and organometallic species of interest.

Keywords: Trapped Ion Mobility Spectrometry; Mass Spectrometry; Organic Gunshot Residue; Inorganic Gunshot Residue.

INTRODUCTION

The discharge of a firearm provides a chemically rich and complex assortment of molecules, typically classified into organic and inorganic gunshot residues (O- and IGSRs), collectively referred to as firearms discharge residue (FDR). FDR is not only composed of species and particulates from the starting material (e.g., primer, propellant, cartridge, projectile jacket, gun barrel and lubricants) but also from combustion and transformation byproducts [1]. The analysis of these species and particulates is pivotal in providing evidence in criminal cases hence much effort has been exerted in developing techniques to collect, identify, and detect them.

Current analytical methods are compartmentalized for the detection of OGSR or GSR. [1, 2] GSR particulates have been traditionally analyzed by scanning electron microscopy electron dispersive X-ray spectroscopy (SEM/EDS) [3]. Alternatively, microbeam ion beam analysis (e.g., m-PIXE) can provide elemental quantitative and more sensitive determination of "characteristic" GSR species. [4] OGSR detection typically includes various pre-separation and extraction techniques (e.g., gas chromatography, liquid chromatography, and solid-phase microextraction) followed by their detection (e.g., electron capture detection, ultraviolet and fluorescence detection, thermal energy analysis, ion mobility, and mass spectrometry). When using multiple assays and complementary techniques (e.g., ATR-FTIR [5], micro-Raman combined with laser ablation ICP-MS [6, 7], LIBS/ICP-OES and GC/μ-ECD and GC/MS [8, 9], SEM/EDS and LC-MS/MS [10-12], SEM/EDS and IBA/µPIXE [4, 13] and TOF-SIMS [14-18]), several reports have shown higher confidence and the need for simultaneous detection of GSR and OGSRs. Recently, we reported on the advantages of high resolution, ion beam-based mass spectrometry imaging combining secondary electron and secondary ion images in order to characterize the firearm discharge from skin swabs based on the morphology and composition of the collected species (i.e., particulates and organic compounds) in a single analysis.[19]

In the current work, we propose as a proof of concept an alternative, facile, high throughput method based on the analysis of skin swab samples for both inorganic and organic species using electrospray trapped ion mobility mass-spectrometry (ESI-TIMS-MS). The proposed method is based on the simultaneous extraction of inorganic and organic species assisted by the formation organometallic complexes (e.g., 15-5 crown ethers for the sequestering of metals and nitrate species), followed by fast, post-ionization, high resolution mobility and mass separations. A key feature is the use of nano-ESI to optimize the transfer of material into the gas phase and utilize small sample volumes (e.g., tens of microliters) for higher sensitivity.

EXPERIMENTAL SECTION

Materials and Reagents

All metal stock standards were single element ICP-MS standards purchased from ULTRA Scientific® (N. Kingstown, Rhode Island) with the exception of potassium which was purchased from SPEX CertiPrep® (Metuchen, New Jersey). 15-crown-5 at 98% purity was purchased from Sigma-Aldrich® (St. Louis, Missouri). Antimony, barium, copper, and lead stock standard solutions were at a concentration of 10,000 µg/mL in water with dilute nitric acid, while potassium was at 1,000 mg/L in 2% nitric acid. The metal charge state in solution was defined by the salt used. A 12,056 ppm stock solution of 15-crown-5 was prepared in HPLC grade methanol (Fisher Chemical, Fair Lawn, New Jersey). The metal stock standards and methanol were used without further purification. The stock metal and crown ether solutions were diluted to working solutions of 3.0 x 10^{-3} M each in methanol. Any additional dilutions were also prepared in the HPLC grade methanol. Other solvents used were acetonitrile and ethyl acetate, LC/MS grade and certified ACS respectively (Fisher Chemical, Fair Lawn, New Jersey). Stock standard solutions of diphenylamine (DPA), ethyl centralite (EC), and 2,4-dinitrotolune (DNT) were prepared at approximately 10 mg/mL from analytical grade solids in methanol (0.2 micron filtered) purchased from Fisher Scientific®.

The sampling media used, CapSure® (Boston, Massachusetts) VP (low particulate clean room wipe), was obtained from Berkshire® (Boston, Massachusetts). The media is 100% knitted polyester and originally 23 cm x 23 cm in size. To allow for easy handling while sampling the media was cut to approximately 4.0 cm x 1.5 cm. The swabs were pre-conditioned prior to use by placing and storing them in a glass jar in a laboratory oven at approximately 80 ºC. Collection of control shooting samples was accomplished by firing 3 shots from a Smith and Wesson 0.38 revolver firearm then wiping both the left and right hands of the shooter with a pre-wetted swab (WVU IRB protocol #1209000337). The swabs were pre-wet with ~ 1 mL of isopropyl alcohol prior to thorough wiping of the top and palm of the hand and the crease between the index finger and thumb. Both hands were sampled on the same swab which was then placed in a glass tube, capped, and labeled. Swab samples were expose to CE based extraction for the inorganic content and organic extraction for the organic content.

nESI-TIMS-MS analysis

A custom nESI-TIMS unit coupled to an Impact Q-TOF mass spectrometer (Bruker, Billerica, Massachusetts) was used for all the experiments.[20-22] The TIMS unit is controlled by custom software in LabView (National Instruments) synchronized with the MS platform controls.[20] Sample aliquots (<10 μL) of the extracted material in the low micromolar range (~1-15 μM) were loaded in a pulled-tip capillary biased at 700-1200 V to the MS inlet. TIMS separation depends on the gas flow velocity (v_g), elution voltage ($V_{elution}$), ramp time (t_{ramp}) and base voltage (V_{out}).[21, 23] The mobility, K, is defined by:

$$K = \frac{v_g}{E} \cong \frac{A}{(V_{elution} - V_{out})} \tag{1}$$

The mobility calibration constant A was determined using known reduced mobilities of Agilent Tuning Mix (Santa Clara, California) components (K_0 of 1.376, 1.013, and 0.835 $cm^2/(V.s)$ for respective *m/z* 322, 622, and 922) as described in ref [22]. The buffer gas was N_2 at ambient temperature (T) with v_g set by the pressure difference between the funnel entrance (P1 = 2.6 mbar) and exit (P2 = 1.1 mbar). An rf voltage of 230 V_{pp} at 2080 kHz was applied to all electrodes. Ions were softly transferred and injected into the TIMS analyser section injection to avoid collisional induced activation (see TIMS schematics in Figure S1). Peak fronting in the CCS profiles (or tailing in the scan domain) was observed at higher masses was due to poor transmission in the collision cells since the instrument was tuned for low mass ions. A typical analysis consisted of 2,000 IMS-MS spectra, divided in 100 accumulations in 20 frames (i.e., ~3-15 min depending on the t_{trap}). The measured mobilities were converted into collision cross sections (CCS, Å^2) using the Mason-Schamp equation:

$$\Omega = \frac{(18\pi)^{1/2}}{16} \frac{q}{(k_B T)^{1/2}} \left(\frac{1}{m} + \frac{1}{M}\right)^{1/2} \frac{1}{N} \times \frac{1}{K} \tag{2}$$

where *q* is the ion charge, k_B is the Boltzmann constant, *N* is the gas number density, *m* is the ion mass, and *M* is the gas molecule mass.[23]

Theoretical Section

Candidate structures were proposed for the organic and organometallic species observed from the skin swabs. Several initial guess structures were proposed for the crown ether (CE) and metal (Me) complexes, but they mostly converged to ones described here; other initial guesses attempts did not converge. The candidate structures were optimized at DFT/B3LYP/6-31+g(d) level of theory using the electrostatic potential (ESP) for all metals of the organometallic complexes except for potassium using the Gaussian 09 package.[24] Partial atomic charges were calculated using the Merz−Singh−Kollman scheme constrained to the molecular dipole moment.[25, 26] Theoretical ion-neutral collision cross-sections (CCS) were calculated using IMoS [27-29] packages with the trajectory method and the diffuse hard sphere scattering (DHSS) method. In the case of DHSS, a temperature of 304 K, a pressure of 101325 Pa, 3 rotations, and 3 million collisions with N_2 gas molecules were considered; an accommodation (percentage of non-elastic collisions) of 0.70 yielded the best results when compared with the experimental CCS. Details on the optimized geometries can be found in the supplemental information.

RESULTS AND DISCUSSION

The analysis of the skin swab extractions using nESI-TIMS-MS resulted in the observation of multiple single and double charged species (see Figure 1). Closer inspection of Figure 1 permitted the identification of a series of organometallic and organic species simultaneously. In positive ion mode, all the organometallic species were detected, while organic species are detected in positive or negative mode depending on the functional groups of the molecule of interest. The high mass resolution permitted the identification of the metals based on their isotopic pattern and the high mobility separation provided reduced chemical noise and higher peak capacity (see Figure 2 and Table 1). That is, from a single analysis, both organic and organometallic species are detected. One of the advantage of gas-phase, post-ionization separations using TIMS-MS is that a single acquisition takes typically 100 ms (up to 500 ms for the highest mobility resolution R_{IMS}~250), with a total analysis time in the order of few minutes.

The search for organic gunshot residue revealed the presence of diphenylamine and ethyl centralite in positive ion mode as protonated and sodiated species, respectively (Figure 1 and 2). These two compounds are commonly used as stabilizers in smokeless gunpowder. Analysis of the mobility profile showed a single IMS bands for both compounds, which makes them easily identifiable in the IMS-MS domain. In addition, other potential organic components can be observed in negative ion mode as deprotonated species . To illustrate the potential of the proposed nESI-TIMS-MS workflow for their detection a typical IMS and MS profiles of a dinitrotoluene (DNT) standard are shown in Figure 2. DNT is observed in the $[M-H]^-$ form and is commonly used as a plasticizer and burn rate modifier in smokeless gun powder and propellants. A good agreement is observed between the experimental and theoretical CCS of the proposed candidate structures (Figure 2).

The organometallic species composed of the 15-5 crown ether (CE) and a metal (Me) had the general form: $[CE+Me]^{+1}$ with Me = Cu; $[CE+Me+NO_3]^{+1}$ with Me = Ba and Pb; $[CE+Me+CE]^{+1}$ with Me = K; $[CE+Me+CE]^{+2}$ with Me = Ba and Pb; and $[CE+Me+(NO_3)_3+Me+CE]^{+1}$ with Me = Ba and Pb. A single mobility band was observed for all organometallic species, which makes them easily identifiable in the IMS-MS domain. Notice that this approach using organometallic complexes provides similar chemical signatures as those obtained using traditional particulate GSR detection with SEM/EDX. [3]

Candidate structures proposed for all the organometallic species provide insights of the coordination of the CE with the Me and with the nitrate group (see Figure 2).. The pocket size of 15-5 and the ionic radius of the metal determines the observation of $[CE+Me]^{+1}$ and $[CE+Me+CE]^{+1}$ species. For example, $[CE+Me+CE]^{+1}$ species were observed for Me = K and not for Cu. This observation does not stem from the oxidation state of the metal, but from their ionic radius. Copper, with a smaller ionic radius, resides deeper within the pocket of the 15-5 CE (Figure 2a); the copper ion is essentially coplanar with the atoms which make up the CE pocket, thus shielding the copper ion from potential coordination with a second crown ether. The proposed structures are in good agreement with previously reported X-ray structures of $[CE+Me+NO_3]$.[30]

CONCLUSIONS

The analytical power of TIMS-MS for the fast separation and identification of compounds from a complex mixture was used for the detection of organometallic and organic species from skin swabs of firearms gunshot residues. The use of 15-5 crown ether allowed the complexation of a variety of metals and nitrate (Me= Ba^{+2}, Pb^{+2}, Cu^{+}, K^{+}, and NO_3^{-}), that are traditionally used as fingerprints of the gunshot residue. In addition, the observation of organic compounds adds selectivity to the workflow by identification of organic gunshot residues (e.g., diphenylamine, ethyl centralite, and dinitrotoluene). The high mass resolution allowed the clear identification of the compounds based on their mass accuracy and isotopic pattern. Theoretical calculations provided candidate structures for all species observed.

ASSOCIATED CONTENT

Supporting Information

Scheme of the TIMS cell. This material is available free of charge via the Internet at http://pubs.acs.org.

AUTHOR INFORMATION

Corresponding Author

fernandf@fiu.edu

Author Contributions

The manuscript was written through contributions of all authors. All authors have given approval to the final version of the manuscript.

Notes

The authors declare no competing financial interest.

ACKNOWLEDGEMENTS

This work was supported by NSF CAREER (CHE-1654274), with co-funding from the Division of Molecular and Cellular Biosciences to FFL. We will like to acknowledge Dr. Mark E. Ridgeway and Dr. Melvin A. Park support during the development and installation of the custom nESI-TIMS-MS instruments. Work by the WVU researchers was supported by a grant from the US Department of Commerce, National Institute of Standards and Technology (NIST), award number 70NANB16H104

REFERENCES

[1] O. Dalby, D. Butler, J.W. Birkett, Analysis of Gunshot Residue and Associated Materials—A Review, Journal of forensic sciences, 55 (2010) 924-943.

[2] R.V. Taudte, A. Beavis, L. Blanes, N. Cole, P. Doble, C. Roux, Detection of Gunshot Residues Using Mass Spectrometry, BioMed Research International, 2014 (2014) 965403.

[3] A. International, Standard Guide for Gunshot Residue Analysis by Scanning Electron Microscopy/Energy Dispersive X-ray Spectrometry, in, ASTM International, East Conshohocken, PA, 2010.

[4] F.S. Romolo, M.E. Christopher, M. Donghi, L. Ripani, C. Jeynes, R.P. Webb, N.I. Ward, K.J. Kirkby, M.J. Bailey, Integrated Ion Beam Analysis (IBA) in Gunshot Residue (GSR) characterisation, Forensic Science International, 231 (2013) 219-228.

[5] J. Bueno, I.K. Lednev, Attenuated Total Reflectance-FT-IR Imaging for Rapid and Automated Detection of Gunshot Residue, Analytical Chemistry, 86 (2014) 3389-3396.

[6] Z. Abrego, N. Grijalba, N. Unceta, M. Maguregui, A. Sanchez, A. Fernandez-Isla, M. Aranzazu Goicolea, R.J. Barrio, A novel method for the identification of inorganic and organic gunshot residue particles of lead-free ammunitions from the hands of shooters using scanning laser ablation-ICPMS and Raman micro-spectroscopy, Analyst, 139 (2014) 6232-6241.

[7] J.C.D. Freitas, J.E.S. Sarkis, O.N. Neto, S.B. Viebig, Identification of Gunshot Residues in Fabric Targets Using Sector Field Inductively Coupled Plasma Mass Spectrometry Technique and Ternary Graphs*, Journal of forensic sciences, 57 (2012) 503-508.

[8] A. Tarifa, J.R. Almirall, Fast detection and characterization of organic and inorganic gunshot residues on the hands of suspects by CMV-GC-MS and LIBS, Science & justice : journal of the Forensic Science Society, 55 (2015) 168-175.

[9] C. Weyermann, V. Belaud, F. Riva, F.S. Romolo, Analysis of organic volatile residues in 9 mm spent cartridges, Forensic Science International, 186 (2009) 29-35.

[10] J.L. Thomas, D. Lincoln, B.R. McCord, Separation and Detection of Smokeless Powder Additives by Ultra Performance Liquid Chromatography with Tandem Mass Spectrometry (UPLC/MS/MS), Journal of forensic sciences, 58 (2013) 609-615.

[11] D. Laza, B. Nys, J.D. Kinder, A. Kirsch-De Mesmaeker, C. Moucheron, Development of a Quantitative LC-MS/MS Method for the Analysis of Common Propellant Powder Stabilizers in Gunshot Residue*, Journal of forensic sciences, 52 (2007) 842-850.

[12] S. Benito, Z. Abrego, A. Sánchez, N. Unceta, M.A. Goicolea, R.J. Barrio, Characterization of organic gunshot residues in lead-free ammunition using a new sample collection device for liquid chromatography–quadrupole time-of-flight mass spectrometry, Forensic Science International, 246 (2015) 79-85.

[13] M.E. Christopher, J.-W. Warmenhoeven, F.S. Romolo, M. Donghi, R.P. Webb, C. Jeynes, N.I. Ward, K.J. Kirkby, M.J. Bailey, A new quantitative method for gunshot residue analysis by ion beam analysis, Analyst, 138 (2013) 4649-4655.

[14] J. Coumbaros, K.P. Kirkbride, G. Klass, W. Skinner, Characterisation of 0.22 caliber rimfire gunshot residues by time-of-flight secondary ion mass spectrometry (TOF-SIMS): a preliminary study, Forensic Science International, 119 (2001) 72-81.

[15] C.M. Mahoney, G. Gillen, A.J. Fahey, Characterization of gunpowder samples using time-of-flight secondary ion mass spectrometry (TOF-SIMS), For. Sci Int., 158 (2006) 39-51.

[16] M.I. Szynkowska, A. Parczewski, K. Szajdak, J. Rogowski, Examination of gunshot residues transfer using ToF-SIMS, Surface and Interface Analysis, 45 (2013) 596-600.

[17] M.I. Szynkowska, K. Czerski, J. Rogowski, T. Paryjczak, A. Parczewski, Detection of exogenous contaminants of fingerprints using ToF-SIMS, Surf. Interface Anal., 42 (2010) 393-397.

[18] M.I. Szynkowska, K. Czerski, J. Grams, T. Paryjczak, A. Parczewski, Preliminary studies using imaging mass spectrometry TOF-SIMS in detection and analysis of fingerprints, Imaging Sci. J., 55 (2007) 180-187.

[19] A. Castellanos, S. Bell, F. Fernandez-Lima, Characterization of firearm discharge residues recovered from skin swabs using sub-micrometric mass spectrometry imaging, Analytical Methods, 8 (2016) 4300-4305.

[20] F.A. Fernandez-Lima, D.A. Kaplan, M.A. Park, Note: Integration of trapped ion mobility spectrometry with mass spectrometry, Rev. Sci. Instr., 82 (2011) 126106.

[21] F.A. Fernandez-Lima, D.A. Kaplan, J. Suetering, M.A. Park, Gas-phase separation using a Trapped Ion Mobility Spectrometer, Int. J. Ion Mobil. Spectrom., 14 (2011) 93-98.

[22] D.R. Hernandez, J.D. DeBord, M.E. Ridgeway, D.A. Kaplan, M.A. Park, F. Fernandez-Lima, Ion dynamics in a trapped ion mobility spectrometer, Analyst, 139 (2014) 1913-1921.

[23] E.W. McDaniel, E.A. Mason, Mobility and diffusion of ions in gases, John Wiley and Sons, Inc., New York, New York, 1973.

[24] M.J. Frisch, G.W. Trucks, H.B. Schlegel, G.E. Scuseria, M.A. Robb, J.R. Cheeseman, G. Scalmani, V. Barone, G.A. Petersson, H. Nakatsuji, X. Li, M. Caricato, A. Marenich, J. Bloino, B.G. Janesko, R. Gomperts, B. Mennucci, H.P. Hratchian, J.V. Ortiz, A.F. Izmaylov, J.L. Sonnenberg, D. Williams-Young, F. Ding, F. Lipparini, F. Egidi, J. Goings, B. Peng, A. Petrone, T. Henderson, D. Ranasinghe, V.G. Zakrzewski, J. Gao, N. Rega, G. Zheng, W. Liang, M. Hada, M. Ehara, K. Toyota, R. Fukuda, J. Hasegawa, M. Ishida, T. Nakajima, Y. Honda, O. Kitao, H. Nakai, T. Vreven, K. Throssell, J.A.J. Montgomery, J.E. Peralta, F. Ogliaro, M. Bearpark, J.J. Heyd, E. Brothers, K.N. Kudin, V.N. Staroverov, T. Keith, R. Kobayashi, J. Normand, K. Raghavachari, A. Rendell, J.C. Burant, S.S. Iyengar, J. Tomasi, v. Cossi, J.M. Millam, M. Klene, C. Adamo, R. Cammi, J.W. Ochterski, R.L. Martin, K. Morokuma, O. Farkas, J.B. Foresman, D.J. Fox, Gaussian 09, in, Gaussian, Inc., Wallingford CT, 2016.

[25] U.C. Singh, P.A. Kollman, An approach to computing electrostatic charges for molecules, Journal of Computational Chemistry, 5 (1984) 129-145.

[26] B.H. Besler, K.M. Merz, P.A. Kollman, Atomic charges derived from semiempirical methods, Journal of Computational Chemistry, 11 (1990) 431-439.

[27] C. Larriba, C.J. Hogan, Free molecular collision cross section calculation methods for nanoparticles and complex ions with energy accommodation, Journal of Computational Physics, 251 (2013) 344-363.

[28] C. Larriba, C.J. Hogan, Ion Mobilities in Diatomic Gases: Measurement versus Prediction with Non-Specular Scattering Models, The Journal of Physical Chemistry A, 117 (2013) 3887-3901.

[29] C. Larriba-Andaluz, J. Fernández-García, M.A. Ewing, C.J. Hogan, D.E. Clemmer, Gas molecule scattering & ion mobility measurements for organic macro-ions in He versus N 2 environments, Physical Chemistry Chemical Physics, 17 (2015) 15019-15029.

[30] P. C. Junk, J. W. Steed, Crown ether chemistry of the alkaline earth nitrates, Journal of the Chemical Society, Dalton Transactions, (1999) 407-414.

Table 1. Comparison of theoretical and experimental CCS for organic and inorganic gunshot residue.

Organic Gunshot Residue							
Compound	Molecular Ion	Theoretical *m/z*	Observed m/z		Experimental CCS	Theoretical CCS	
Diphenylamine	$[M+H]^+$	170.096	170.097		149.9	$139.6^{\ddagger}$	
Ethyl Centralite	$[M+Na]^+$	291.146	291.141		167.3	$171.5^{\ddagger}$	
Dinitrotoluene	$[M-H]^-$	181.025	181.025		140.8	$127.4^{\ddagger}$	
Inorganic Gunshot Residue							
Ion Species	Ionic Radius of Metal (pm)	Theoretical *m/z*	Observed m/z		Experimental CCS	Theoretical CCS	
$[CE+Ba+NO_3^-]^+$	1.49	420.023	420.023		167.4	$163.6^{\dagger}$	
$[CE+Pb+NO_3^-]^+$	1.33	490.095	490.095		159.2	$163.2^{\dagger}$	
$[CE+Cu]^+$	0.91	283.060	283.060		140.8	$147.4^{\dagger}$	
$[CE+Ba+CE]^{+2}$	1.49	289.083	289.084		231.3	$224.5^{\ddagger}$	
$[CE+Pb+CE]^{+2}$	1.33	324.119	324.118		229.7	$222.3^{\ddagger}$	
$[CE+K+CE]^+$	1.52	479.225	479.225		186.1	$180.7^{\ddagger}$	
†Diffuse Hard Sphere Scattering (DHSS) ‡Trajectory Method (TM)							

Figure 1. Typical 2D-IMS-MS contour plots obtained in positive (a) and negative (b) ion modes.

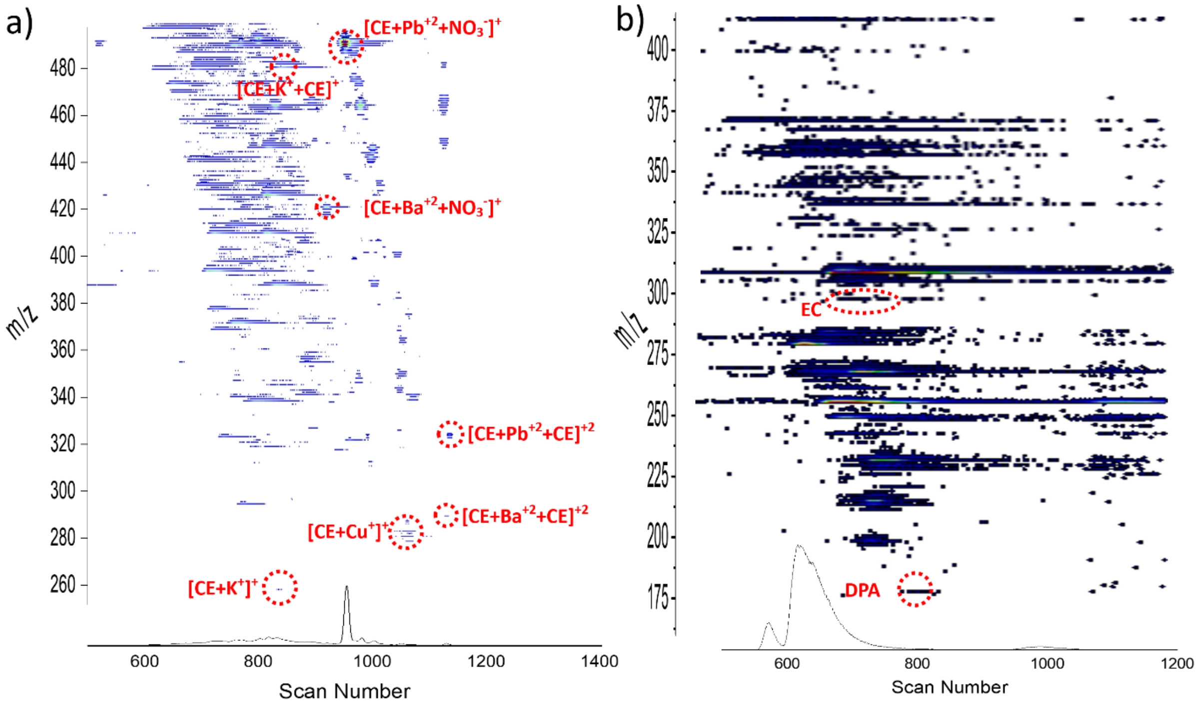

Figure 2. TIMS mobility profiles with theoretical structure and mass spectrum as an inset.